First Example of a Reversible Single-Crystal-to-Single-Crystal Polymerization−Depolymerization Accompanied by a Magnetic Anomaly for a Transition-Metal Complex with an Organic Radical

Victor I. Ovcharenko,* Sergey V. Fokin, Elvina T. Kostina, Galina V. Romanenko, Artem S. Bogomyakov, and Eugene V. Tretyakov

International Tomography Center, Russian Academy of Sciences, 3A Institutskaya Str., 630090 Novosibirsk, Russian Federation

S *Supporting Information*

ABSTRACT: The reaction of copper(II) hexafluoroacetyla-cetonate $[Cu(hfac)_2]$ with the stable nitronyl nitroxide 2-(1-ethyl-3-methyl-1*H*-pyrazol-4-yl)-4,4,5,5-tetramethyl-4,5-dihydro-1*H*-imidazole-3-oxide-1-oxyl (L^a) resulted in a paired heterospin complex $[[Cu(hfac)_2]_3(\mu\text{-}O,N\text{-}L^a)_2][Cu(hfac)_2(O\text{-}L^a)_2]$. The crystals of the compound were found to be capable of a reversible single-crystal-to-single-crystal (SC−SC) transformation initiated by the variation of temperature. At room temperature, the molecular structure of $[[Cu(hfac)_2]_3(\mu\text{-}O,N\text{-}L^a)_2][Cu(hfac)_2(O\text{-}L^a)_2]$ is formed by the alternating fragments of the pair complex. Cooling the crystals of the complex below 225 K caused considerable mutual displacements of adjacent molecules, which ended in a transformation of the molecular structure into a polymer chain structure. A reversible topotactic polymerization−depolymerization coordination reaction actually takes place in the solid during repeated cooling−heating cycles: $[[Cu(hfac)_2]_3(\mu\text{-}O,N\text{-}L^a)_2][Cu(hfac)_2(O\text{-}L^a)_2] \rightleftharpoons Cu(hfac)_2(\mu\text{-}O,N\text{-}L^a)]_\infty$. Polymerization during cooling is the result of the anomalously great shortening of intermolecular distances (from 4.403 Å at 295 K to 2.460 Å at 150 K; Δd = 1.943 Å) between the terminal Cu atoms of the trinuclear fragments $\{[[Cu(hfac)_2]_3(\mu\text{-}O,N\text{-}L^a)_2]\}$ and the noncoordinated N atoms of the pyrazole rings of the mononuclear $\{[Cu(hfac)_2(O\text{-}L^a)_2]\}$ fragments. When the low-temperature phase was heated above 270 K, the polymer chain structure was destroyed and the compound was again converted to the pair molecular complex. The specifics of the given SC−SC transformation lies in the fact that the process is accompanied by a magnetic anomaly, because the intracrystalline displacements of molecules lead to a considerable change in the mutual orientation of the paramagnetic centers, which, in turn, causes modulation of the exchange interaction between the odd electrons of the Cu^{2+} ion and nitroxide. On the temperature curve of χT, this shows itself as a hysteresis loop. The nontrivial character of the recorded spin transition during the cooling of the sample below 225 K lies in the fact that the magnetic moment abruptly increased. In contrast, heating the sample above 270 K led to a drastic decrease in χT. This behavior of χT is caused by a stepwise change in the character of the exchange interaction in the $\{>N\text{-}^\bullet O\text{-}Cu^{2+}\text{-}O^\bullet\text{-}N<\}$ fragments. The lengthening of distances between the paramagnetic centers on cooling below 225 K led to a transition from antiferromagnetic to ferromagnetic exchange and, vice versa, the shortening of distances between the paramagnetic centers during the heating of the heterospin polymer above 270 K led to a transition from ferromagnetic exchange to antiferromagnetic exchange.
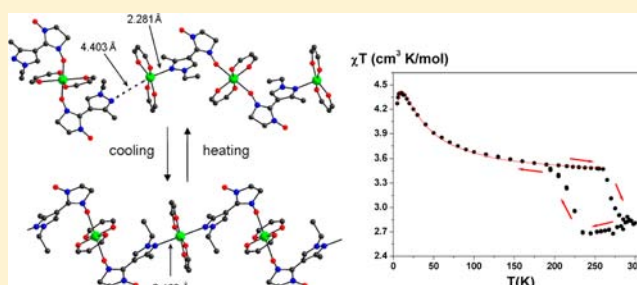
■ INTRODUCTION

Despite great interest in single-crystal-to-single-crystal (SC−SC) transformations,[1−3] examples of compounds of new types capable of such topotactic reactions are rare, because SC−SC processes require high cooperativity and coherence of intracrystalline molecular motions.[4,5] These compounds, however, are of considerable interest for revealing the fundamental relationship between the molecular motion at the microlevel initiated by the external stimuli and the effects of this motion on the crystal as a nano[6,7] or macro object.[8−11] Solids capable of SC−SC transformations are promising as microactuators, molecular sensors, and adjustable molecular switches.[12−19]

Studies of the SC−SC reaction are valuable for elaborating the molecular machinery methods.[20]

Considerable progress in studies of SC−SC transformations was achieved for organic crystals in which the external action (variation of temperature or pressure, irradiation, or treatment of crystal with vapors of small molecules) could initiate isomerization, cyclization, dimerization, polymerization, or sorption.[19,21−25] For coordination compounds, SC−SC transformations were recorded more rarely.[26,27] These SC−SC transformations were mostly accompanied by a loss of solvate

molecules caused by the gentle heating of the single crystal (the reverse solvation occurs after the sample was cooled and kept in solvent vapors).[27−34] SC−SC transformations in which small molecules could be varied in the coordination sphere of the metal were reported even less frequently.[35−37] A special group involves SC−SC polymerizations−depolymerizations of coordination compounds in which the composition of the solid does not change. The formation or cleavage of the metal−ligand bond is caused by the intraphase approach or removal of the metal atom of one molecule and the donor atom of the neighboring molecule.[38−40] In this case, molecules can experience considerable displacements in the single crystal, which retains its integrity; the displacements are reliably recorded in a series of X-ray studies of the same crystal. These processes are generally initiated by heating a crystal above the room temperature. However, an example of an SC−SC transformation initiated by cooling the sample is known; the polymer chain structure of $[ZnCl_2(\mu\text{-bipy})]_\infty$ single crystals was transformed into the layered structure of $[Zn(\mu\text{-Cl})_2(\mu\text{-bipy})]_\infty$ at $T < 130$ K, as a result of the transformation of the terminal Cl atoms into bridging atoms.[40] This reversible SC−SC polymerization−depolymerization was recorded for a transition-metal complex with an organic radical $[[Cu(hfac)_2]_3(\mu\text{-}O,N\text{-}L^a)_2][Cu(hfac)_2(O\text{-}L^a)_2]$, where $Cu(hfac)_2$ is copper(II) hexafluoroacetylacetonate and L^a is the stable nitronyl nitroxide 2-(1-ethyl-3-methyl-1H-pyrazol-4-yl)-4,4,5,5-tetramethyl-4,5-dihydro-1H-imidazole-3-oxide-1-oxyl. Solid $[[Cu(hfac)_2]_3(\mu\text{-}O,N\text{-}L^a)_2][Cu(hfac)_2(O\text{-}L^a)_2]$ has a molecular structure at room temperature. Its cooling, however, caused substantial mutual displacements of the atoms of the neighboring molecules, which led to a complete transformation of the molecular structure of the complex into a polymer chain structure.

The specifics of this SC−SC transformation lies in the fact that the process is accompanied by a magnetic anomaly, because the intracrystalline displacement of molecules led to a significant change in the mutual orientation of the paramagnetic centers, which caused modulation of the exchange interaction between the odd electrons of the Cu^{2+} ion and the nitroxide. Comprehensive data on the structure of the solid before and after its transformation and in the course of it are extremely valuable for understanding the magnetostructural correlations inherent in multispin compounds, because revealing these correlations allows the development of methods for controlled chemical modification of the physical characteristics of the substances.[41]

■ EXPERIMENTAL SECTION

General Procedures. 3-Methyl-1H-pyrazole[42] and 2,3-bis(hydroxyamino)-2,3-dimethylbutane sulfate monohydrate[43,44] were synthesized as described in the literature. Commercial reagents and solvents were used without additional purification. The progress of the reactions was monitored by TLC on silica gel 60 F_{254} aluminum sheets (Merck). A chromatographic study was carried out using silica gel (0.063−0.200 mm, Merck) for column chromatography. The infrared spectrum of nitroxide L^a (4000−400 cm^{-1}) was recorded with a VECTOR 22 Bruker instrument for a KBr pellet. Microanalysis was carried out on an EA-3000 HEKAtech GmbH analyzer.

Synthesis of the Ligand. Author: A mixture of 1-ethyl-3-methyl-pyrazole (**1a**) and 1-ethyl-5-methyl-1H-pyrazole[45] (**1b**) was obtained from 3-methyl-1H-pyrazole using EtI and 40% KOH by a procedure similar to that described in the literature.[46] According to NMR data, the ratio of **1a** to **1b** in the reaction product was ∼7/3 (the lines were assigned using the reference ^{1}H NMR spectrum of **1a**[47]). The mixture

of **1a** and **1b** could not be separated by traditional methods until L^a and L^b were obtained.

a, R = 3-Me
b, R = 5-Me
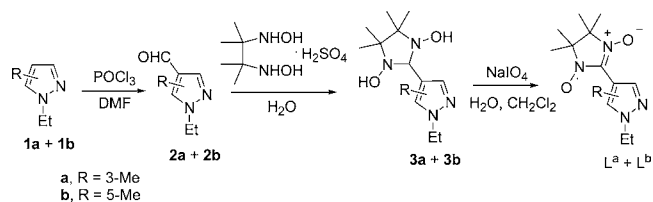
2-(1-Ethyl-3-methyl-1H-pyrazol-4-yl)- (L^a) and 2-(1-ethyl-5-methyl-1H-pyrazol-4-yl)-4,4,5,5-tetramethyl-4,5-dihydro-1H-imidazole-3-oxide-1-oxyl (L^b). $POCl_3$ (6.0 mL, 0.17 mol) was added dropwise for 0.5 h to a solution of **1a** and **1b** (7.80 g, 70.8 mmol) in DMF (16 mL) stirred at 100 °C. The reaction mixture was stirred for 1 h and cooled. A 20% KOH solution was added to it until pH became ∼10 and then treated with (4 × 10 mL) portions of CH_2Cl_2. The combined organic extracts were dried over Na_2SO_4, filtered through a silica gel layer, and evaporated to give a mixture of aldehydes **2a** and **2b**. 2,3-Bis(hydroxyamino)-2,3-dimethylbutane sulfate hydrate (13.5 g, 51.3 mmol) and water (60 mL) were added to the resulting mixture of isomers **2a** and **2b** (7.0 g, 50.7 mmol). The reaction mixture was stirred at room temperature for 1.5 h. The solution was neutralized with $NaHCO_3$. The precipitate (a mixture of **3a** and **3b**) was filtered off, washed with water and acetone, and dried under vacuum. $NaIO_4$ (4.73 g, 22.1 mmol) was added in portions for 0.5 h to a suspension of **3a** and **3b** (7.42 g, 27.6 mmol) in water (50 mL) and CH_2Cl_2 (100 mL) stirred at ∼5 °C. The cooling was removed and the reaction mixture was stirred for another 1 h. The organic phase was separated and the aqueous phase was extracted with CH_2Cl_2. The combined organic extracts were dried over Na_2SO_4, filtered through an Al_2O_3 layer, and concentrated under vacuum. The oil-like residue was ground with hexane while cooling. This gave a mixture of L^a and L^b in the form of dark-blue fine powder (yield = 1.84 g, 11% based on 3-methyl-1H-pyrazole). Recrystallization of this powder from hexane led only to dark-green platelike crystals of L^a, according to X-ray diffraction (XRD) and infrared (IR) spectroscopy; mp 129−130 °C; TLC: R_f = 0.08 with ethyl acetate on silica gel 60 F_{254} (aluminum sheets, Merck). IR: ν = 3110, 3090, 2979, 2935, 1734, 1593, 1510, 1443, 1397, 1358, 1223, 1174, 1146, 1117, 1083, 1002, 954, 863, 831, 766, 710, 684, 653, 616 cm^{-1}. The product χT was 0.375 ± 0.02 cm^3 K/mol at 100−300 K. $C_{13}H_{22}N_4O_2$ (266.34): calcd. C, 58.6; H, 8.3; N, 21.0; found C, 58.3; H, 7.9; N, 21.4. Further concentration and cooling of the mother solution caused crystallization into the dark-blue needle crystals of L^b. Mp 98−99 °C IR: ν = 2985, 2940, 1597, 1507, 1455, 1399, 1362, 1310, 1221, 1188, 1166, 1144, 1083, 1039, 970, 943, 872, 846, 826, 757, 719, 677, 661, 614 cm^{-1}. $C_{13}H_{22}N_4O_2$ (266.34): calcd. C, 58.6; H, 8.3; N, 21.0; found C, 58.5; H, 7.9; N, 21.3.

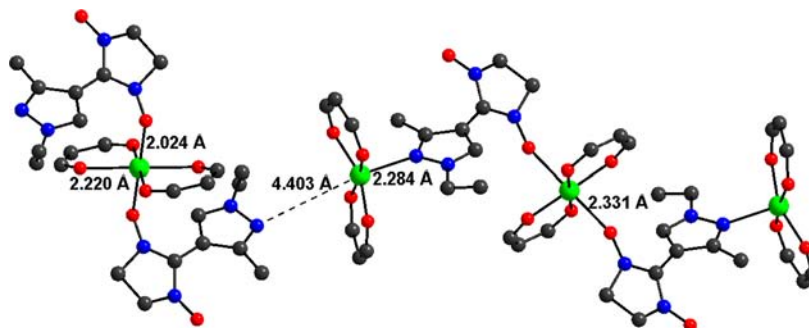**Synthesis of $[[Cu(hfac)_2]_3(\mu\text{-}O,N\text{-}L^a)_2][Cu(hfac)_2(O\text{-}L^a)_2]$.** $Cu(hfac)_2$ (89.6 mg, 18.8 mmol) and L^a (50 mg, 18.8 mmol) were dissolved in ether (2 mL). Hexane (7 mL) was added. The resulting dark-brown solution was kept in an open flask at 25 °C for 4−6 h and then at −5 °C for another 15−20 h. The dark-brown crystals suitable for an XRD analysis were filtered off, washed with hexane, and dried in air. The product is readily soluble in diethyl ether, THF, and acetone, but almost insoluble in benzene and saturated hydrocarbons. Yield = 70%. $Cu_4C_{92}H_{92}N_{16}O_{24}F_{48}$ (2971.92): calcd. C 37.1; H 3.1; N 7.5; F 30.7; found C 37.2; H 3.3; N 8.0; F 30.3.

Note 1. During the synthesis of the complex, storing the reaction mixture for a long time at room temperature can be avoided; instead, the solvent is removed with an air current right after the reagents are mixed, the residue is dissolved in hexane, and the resulting solution is kept at approximately −20 °C overnight. This procedure affords the compound with the same yield (70%).

Note 2. The mixture of L^a and L^b obtained as described above is enriched with L^a. It cannot be separated into components by chromatography on different supports. However, the individual L^a can be isolated by recrystallization of the mixture of L^a and L^b from hexane. Our experiments showed that, in order to avoid a considerable

Table 1. Selected Bond Lengths and Angles for $[[Cu(hfac)_2]_3(\mu\text{-}O,N\text{-}L^a)_2][Cu(hfac)_2(O\text{-}L^a)_2]$, $[Cu(hfac)_2(\mu\text{-}O,N\text{-}L^a)]_\infty$, and $[[Cu(hfac)_2]_3(\mu\text{-}N,O\text{-}L^a)_2]$

	$[Cu(hfac)_2(\mu\text{-}O,N\text{-}L^a)]_\infty$	$[[Cu(hfac)_2]_3(\mu\text{-}O,N\text{-}L^a)_2][Cu(hfac)_2(O\text{-}L^a)_2]$		$[[Cu(hfac)_2]_3(\mu\text{-}N,O\text{-}L^a)_2]$
	T = 150 K	T = 240 K	T = 295 K	T = 240 K
space group, Z	$P\bar{1}$, 2	$P\bar{1}$, 1		$P2_1/n$, 2
Cu−O$_{NO}$ (Å)	2.336(7)	1.981(2)	2.024(2)	1.9320(15)
		2.313(2)	2.331(2)	
Cu−N (Å)	2.460(9)	2.273(3)	2.284(3)	2.549(2)
		4.357(5)	4.403(5)	
∠CuON (°)	131.7(6)	126.6(2)	127.5(2)	119.9(1)
		154.7(2)	154.7(2)	
N−O (Å)	1.302(10) 1.265(10)	1.311(3), 1.274(3)	1.309(3), 1.268(3)	1.312(2), 1.271(2)
		1.281(3), 1.275(3)	1.282(3), 1.273(3)	
−•O⋯O•− (Å)	3.913	3.708	3.758	>7

Figure 1. Structure of the trinuclear and mononuclear molecules of the pair complex and their mutual arrangement in crystal (T = 295 K).

loss of L^a during the synthesis of $[[Cu(hfac)_2]_3(\mu\text{-}O,N\text{-}L^a)_2][Cu(hfac)_2(O\text{-}L^a)_2]$, we can use an unseparated mixture of L^a and L^b. When it is used instead of pure L^a, only $[[Cu(hfac)_2]_3(\mu\text{-}O,N\text{-}L^a)_2][Cu(hfac)_2(O\text{-}L^a)_2]$ solid crystals are isolated under the given conditions.

Note 3. Reproductions of the synthesis of $[[Cu(hfac)_2]_3(\mu\text{-}O,N\text{-}L^a)_2][Cu(hfac)_2(O\text{-}L^a)_2]$ occasionally gave solid impurity crystals of the trinuclear $[[Cu(hfac)_2]_3(\mu\text{-}N,O\text{-}L^a)_2]$ complex, along with the desired product. For this reason, each newly synthesized batch of the pair complex should be checked. Since the $[[Cu(hfac)_2]_3(\mu\text{-}O,N\text{-}L^a)_2][Cu(hfac)_2(O\text{-}L^a)_2]$ (elongated rhombohedra) and $[[Cu(hfac)_2]_3(\mu\text{-}N,O\text{-}L^a)_2]$ (prisms) crystals have different shapes, the formation of an impurity phase can be monitored with a microscope.

Synthesis of $[[Cu(hfac)_2]_3(\mu\text{-}N,O\text{-}L^a)_2]$. Cu(hfac)$_2$ (71.6 mg, 15 mmol) and diethyl ether (2 mL) were added to a mixture of L^a and L^b (26.6 mg, 10 mmol). Hexane (7 mL) was added to the resulting dark-brown solution and the surface of the reaction mixture was blown with an air current for 2 h. The volume of the mixture decreased by more than one-half and the ether odor vanished. The reaction mixture was kept overnight at −5 °C. The dark brown crystals suitable for an XRD analysis were filtered off, washed with hexane, and dried in air. The complex is readily soluble in diethyl ether, THF, and acetone and almost insoluble in benzene and saturated hydrocarbons. Yield = 75%. Cu$_3$C$_{56}$H$_{48}$N$_8$O$_{16}$F$_{36}$ (1963.61): calcd. C 34.3; H 2.5; N 5.7; F 33.8; found C 34.6; H 2.5; N 5.8; F 33.7.

X-ray Crystallography. The intensity data for the single crystals of L^a, L^b, $[[Cu(hfac)_2]_3(\mu\text{-}O,N\text{-}L^a)_2][Cu(hfac)_2(O\text{-}L^a)_2]$, and $[[Cu(hfac)_2]_3(\mu\text{-}N,O\text{-}L^a)_2]$ were collected on a SMART APEX CCD (Bruker AXS) automated diffractometer with a Helix (Oxford Cryosystems) open flow helium cooler using the standard procedure (Mo Kα radiation). The structures were solved by direct methods and refined by the full-matrix least-squares procedure anisotropically for non-hydrogen atoms. The H atoms were partially located in difference electron density syntheses or calculated geometrically and included in the refinement as riding groups. All calculations were fulfilled with the SHELXTL 6.14 program package. The temperature dynamics of the selected structural parameters for the complexes is presented in Table 1.

Note that the preparation of perfect crystals of $[[Cu(hfac)_2]_3(\mu\text{-}O,N\text{-}L^a)_2][Cu(hfac)_2(O\text{-}L^a)_2]$ requires a certain technology. Since the compound is very well soluble, even in low-polar organic solvents at room temperature, its mother solution should be cooled for crystallization. As shown by numerous experiments on single crystal growth, however, the cooling should be moderate. The mother solution should not be cooled below 255−260 K, because the resulting single crystals are unstable upon heating and start to crack, even in solution. After the crystals are separated from the mother solution, they crack even more significantly and become almost unsuitable for diffraction studies. The crystals prepared without overcooling can be stored in a refrigerator and do not lose their quality for a long time. A complete XRD study can be performed for such crystals in different states at different temperatures. We wanted to study the structure of the compound at different temperatures for the same crystal, but the structural transition due to the variation of temperature always led to partial (more or less significant) decomposition of the single crystal. The associated CIF files (in the Supporting Information) give the structural data discussed in the text and obtained in diffraction experiments at 240 and 150 K for the same single crystal. The results of the structural study at 295 K are given for another crystal, because repeated heating of the crystal studied initially at 240 and 150 K markedly degraded its quality (caused its cracking), even though the crystal was covered with an epoxide layer before the experiment.

Magnetic Measurements. Magnetic measurements were carried out on an MPMS*XL* SQUID magnetometer (Quantum Design) in the
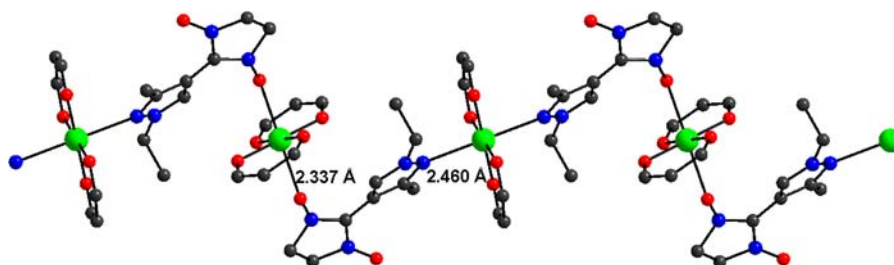
Figure 2. Fragment of the polymer chain of $[Cu(hfac)_2L^a]_\infty$ (T = 150 K).

temperature range of 2−300 K in a magnetic field of up to 5 kOe. The molar magnetic susceptibility was calculated using diamagnetic corrections for the complexes according to the Pascal scheme. The experimental temperature dependences of χT were calculated for the $\{Cu(hfac)_2L^a\}_4$ unit for $[[Cu(hfac)_2]_3(\mu\text{-}O,N\text{-}L^a)_2][Cu(hfac)_2(O\text{-}L^a)_2]$ and $[Cu(hfac)_2(\mu\text{-}O,N\text{-}L^a)]_\infty$. For this complex, which exhibited abrupt magnetic and structural phase transitions, measurements of $\chi T(T)$ were performed at decreasing and increasing temperature. The magnetic data had good reproducibility for different batches of the compound and hysteresis was revealed.

■ RESULTS AND DISCUSSION

The interaction of $[Cu(hfac)_2]$ with L in a diethyl ether−hexane mixture at a 1:1 ratio of reagents allowed a reproducible synthesis of the polycrystalline phase, whose composition corresponded to the formula $Cu(hfac)_2L^a$ according to the element analysis data. An XRD study of the crystals performed at 295 K showed that they were formed by the alternating molecules of the $[[Cu(hfac)_2]_3(\mu\text{-}O,N\text{-}L^a)_2][Cu(hfac)_2(O\text{-}L^a)_2]$ pair complex (see Figure 1).

Both the trinuclear $[[Cu(hfac)_2]_3(\mu\text{-}O,N\text{-}L^a)_2]$ and mononuclear $[Cu(hfac)_2(O\text{-}L^a)_2]$ molecules of the pair complex are centrosymmetric. The vertices of the square bipyramid of the central Cu atom of the $[[Cu(hfac)_2]_3(\mu\text{-}O,N\text{-}L^a)_2]$ trinuclear molecule are occupied by the O atoms of the NO groups (Cu−O_{NO} = 2.331(2) Å; see Table 1). The N donor atoms of L^a occupy the vertices of the square pyramids at the terminal Cu atoms (2.284(3) Å). In the mononuclear $[Cu(hfac)_2(O\text{-}L^a)_2]$ molecule, the paramagnetic ligands are coordinated only by the O_{NO} atoms. The Cu−O_{NO} distances are short (2.024(2) Å), because the axial positions in the bipyramid are occupied by the O atoms of the hfac anions ($d_{Cu-Ohfac}$ = 2.220(3) Å). Also note that the CuON angles in the molecules are different: 154.7(2)° in the trinuclear molecule and 127.5(2)° in the mononuclear one. The shortest −●O···O●− intermolecular distance between the paramagnetic centers of the neighboring molecules is 3.758(4) Å. The distance from the terminal Cu atoms of the trinuclear molecule to the N atom of the pyrazole ring of L^a in the mononuclear complex is 4.403(5) Å. No similar structures were reported earlier in the series of metal compounds with nitroxides of the heterospin phase.[48]

When the crystal was cooled to 240 K, our XRD experiment recorded only a small shortening of all interatomic distances and insignificant changes in the angles (Table 1). The cooling of the $[[Cu(hfac)_2]_3(\mu\text{-}O,N\text{-}L^a)_2][Cu(hfac)_2(O\text{-}L^a)_2]$ crystal from 295 K to 240 K actually caused its insignificant thermal compression.

Further cooling induced a structural rearrangement and a magnetic phase transition. Since the intracrystalline rearrangements were very significant, the $[[Cu(hfac)_2]_3(\mu\text{-}O,N\text{-}L^a)_2]^-$ $[Cu(hfac)_2(O\text{-}L^a)_2]$ crystals cooled below 225 K often cracked. In some experiments, however, their quality remained sufficient

for an XRD study and allowed us to study the structure of both high- and low-temperature phases using the same crystal.

When $[[Cu(hfac)_2]_3(\mu\text{-}O,N\text{-}L^a)_2][Cu(hfac)_2(O\text{-}L^a)_2]$ was cooled, its molecular structure transformed to a polymer chain structure $[Cu(hfac)_2(\mu\text{-}O,N\text{-}L^a)]_\infty$ with a "head-to-head" motif as a result of the phase transition (Figure 2). When the low-temperature phase was heated above 270 K, the polymer chain structure decomposed and the compound again transformed to a molecular pair complex. Thus, a thermally induced reversible chemical reaction of coordination polymerization−depolymerization $[[Cu(hfac)_2]_3(\mu\text{-}O,N\text{-}L^a)_2][Cu(hfac)_2(O\text{-}L^a)_2]$ $\rightleftharpoons [Cu(hfac)_2(\mu\text{-}O,N\text{-}L^a)]_\infty$ occurs in the multispin solid under study in the course of repeated cooling−heating cycles.

A comparison of the structures of the low- and high-temperature phases revealed numerous displacements of molecules during the transition in the crystals. The distance between the terminal Cu atom of the trinuclear molecule and the pyrazole N atom of L^a of the mononuclear molecule in the high-temperature phase experienced the greatest change. It was shortened by more than 1.9 Å, compared to the same distance at 295 K. As a result, the terminal Cu atom of the trinuclear molecule moved from its position in the inner space of the surrounding square pyramid to the pyramid base; its environment was completed to centrosymmetric bipyramidal, which was due to the N atom of the pyrazole ring of the neighboring $[Cu(hfac)_2(O\text{-}L^a)_2]$ molecule. A comparison of Figures 1 and 2 shows that the Cu−N distance, which is 4.403(5) Å in Figure 1, decreases to 2.460(9) Å. The solid-state process under study is thus reversible coordination polymerization−depolymerization, because the Cu−N bond appears when the high-temperature phase is cooled below 225 K and is broken when the low-temperature phase is heated above 270 K.

The distance between the terminal Cu atom of the trinuclear molecule and the pyrazole N atom of L^a of the mononuclear molecule of the high-temperature phase was considerably shortened, while the Cu−O_{NO} distances in the coordination sphere of the central Cu atom in the former trinuclear molecule were slightly elongated upon passing to the low-temperature phase. The distances are 2.331(2) Å (295 K, Figure 1) and 2.313(2) Å (240 K) in the high-temperature phase and 2.336(7) Å in the low-temperature phase (150 K, Figure 2). In the former mononuclear $[Cu(hfac)_2(O\text{-}L^a)_2]$ molecules, the Cu−O_{NO} distances increased much more drastically, as a result of solid-state polymerization (2.024(2) (295 K, Figure 1), 1.981(2) Å at 240 K, and 2.336(7) Å at 150 K (Figure 2)). The considerable lengthening of these distances causes a significant rearrangement of the environment in the CuO_6 units. As a result, the structural characteristics are equalized in all CuO_6 units of the $[Cu(hfac)_2(\mu\text{-}O,N\text{-}L^a)]_\infty$ polymer chain, with the

O atoms of the coordinated nitronyl nitroxyl groups lying on the elongated $O_{NO}-Cu-O_{NO}$ Jahn−Teller axis in these units.

The thermally induced reaction leads to great changes in the distances of $\{>N-{}^{\bullet}O-Cu^{2+}-O^{\bullet}-N<\}$ exchange clusters and is accompanied by a magnetic anomaly on the temperature dependence of χT (Figure 3). The structural rearrangement of
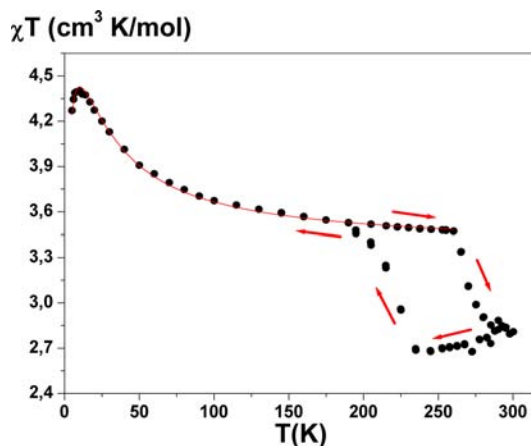

Figure 3. Dependence $\chi T(T)$ for $[[Cu(hfac)_2]_3(\mu\text{-}O,N\text{-}L^a)_2][Cu(hfac)_2(O\text{-}L^a)_2]$ (data points represent experimental values; solid line denote the theoretical curve). The arrows indicate the direction of variation of χT during the cooling and subsequent heating of the sample.

the complex leads to a spin transition, which shows itself as a hysteresis loop on the $\chi T(T)$ curve during the cooling−heating cycle. The nontriviality of the spin transition lies in the fact that χT jumps upon cooling below 225 K, but drastically decreases upon heating above 270 K. This behavior of χT is explained by a change in the character of the exchange interaction in the $\{>N-{}^{\bullet}O-Cu^{2+}-O^{\bullet}-N<\}$ fragments from antiferromagnetic to ferromagnetic upon cooling and, vice versa, from ferromagnetic to antiferromagnetic upon heating.

When the high-temperature phase was cooled from 300 K to ~235 K, χT decreased from 2.82 cm^3 K/mol to 2.69 cm^3 K/mol, then abruptly increased to 3.47 cm^3 K/mol at 195 K, and increased smoothly, reaching its maximum (4.40 cm^3 K/mol) at 10 K (Figure 3). During the reverse cycle, the curve was repeated in the range 10−195 K. Further heating, however, led to a drastic decrease in χT above 270 K. Upon heating from 270 K to 295 K, χT decreased from 3.47 cm^3 K/mol to 2.72 cm^3 K/mol.

In the course of the heating of the low-temperature phase from 10 K to 270 K, χT tends toward 3.37 cm^3 K/mol, which corresponds to a system of eight weakly interacting centers with spin $^1/_2$ and g = 2.12. We took the latter value as an estimated mean between the g-factor of Cu^{2+} and that of L^a. The form of the $\chi T(T)$ curve in the range from 10 K to 270 K indicates that the ferromagnetic exchange interactions are dominant. Theoretical treatment of the curve $\chi T(T)$ in the temperature range of 10−260 K, using the exchange cluster model,[49] gave the following optimum values of parameters: g_R = 2 (fixed), g_{Cu} = 2.23 ± 0.01, J = 20.7 ± 0.4, zJ' = −0.20 ± 0.01. For the three-spin exchange cluster $\{>N-{}^{\bullet}O-Cu^{2+}-O^{\bullet}-N<\}$, the isotropic spin Hamiltonian $H = -2J(S_{R1}S_{Cu} + S_{Cu}S_{R2})$ was used. The contribution of the Cu^{2+} ions of the $\{N-Cu^{2+}-N\}$ units to the magnetic susceptibility was taken into account, using the Curie law. The final equation for the magnetic susceptibility is

$$\chi = \chi'_{R-Cu-R} + \frac{C}{T}$$

where χ_{R-Cu-R} is the magnetic susceptibility of the $\{>N-{}^{\bullet}O-Cu^{2+}-O^{\bullet}-N<\}$ three-spin exchange cluster,

$$\chi_{R-Cu-R} = \frac{N\mu_B^2}{4kT}$$

$$\times \frac{10(g_{Cu} + 2g_R)^2 e^{J/(kT)} + (4g_R - g_{Cu})^2 e^{-2J/(kT)} + g_{Cu}^2}{2e^{J/(kT)} + e^{-2J/(kT)} + 1}$$

and χ'_{R-Cu-R} is the magnetic susceptibility of the three-spin exchange cluster, including the intercluster interactions:

$$\chi'_{R-Cu-R} = \frac{\chi_{R-Cu-R}}{1 - \left(\frac{4zJ' \chi_{R-Cu-R}}{3}\right)}$$

It is difficult to determine the exchange interaction energy of the high-temperature phase from experimental data, because of the narrow temperature range of the experimental χT values and very strong antiferromagnetic exchange interactions in the $\{>N-{}^{\bullet}O-Cu^{2+}-O^{\bullet}-N<\}$ exchange clusters of the $[Cu(hfac)_2(O\text{-}L^a)_2]$ molecules. Estimation of χT for a system of six weakly interacting paramagnetic centers (admittedly, two spins in the $\{>N-{}^{\bullet}O-Cu^{2+}-O^{\bullet}-N<\}$ exchange clusters of $[Cu(hfac)_2(O\text{-}L^a)_2]$ molecules completely compensate each other; i.e., the ground state of the exchange cluster is a doublet[49]) with a spin = $^1/_2$ and g-factor = 2.12, which gave a value of 2.53 cm^3 K/mol, which agrees well with the experimental χT values in the temperature range of 235−300 K. The experimentally observed hysteresis on the $\chi T(T)$ curve, which corresponds to the reverse solid-state reaction $[[Cu(hfac)_2]_3(\mu\text{-}O,N\text{-}L^a)_2][Cu(hfac)_2(O\text{-}L^a)_2] \rightleftharpoons [Cu(hfac)_2(\mu\text{-}O,N\text{-}L^a)]_\infty$, is reproduced during the repeated cooling−heating cycles. Note that, in the case of the classical spin-crossover,[50−60] the structural changes in the environment of the Fe ion upon passing from a low-spin state to a high-spin state are insignificant.[61]

Attempts to obtain solids from $[Cu(hfac)_2]$ and L^a consisting of the individual components of the $[[Cu(hfac)_2]_3(\mu\text{-}O,N\text{-}L^a)_2][Cu(hfac)_2(O\text{-}L^a)_2]$ pair cluster failed. When the starting ratio of components was L^a/$[Cu(hfac)_2] \geq 2$, we did not isolate any heterospin products. When the $[Cu(hfac)_2]$/L^a ratio was 3/2, a solid heterospin complex with exactly the same ratio $[[Cu(hfac)_2]_3(\mu\text{-}N,O\text{-}L^a)_2]$ was reproducibly isolated. Its molecular crystal structure was indeed formed by trinuclear molecules. In these molecules, however, L^a was coordinated in a different way, compared with the trinuclear molecules of the pair cluster (Figure 4).

In the centrosymmetric $[[Cu(hfac)_2]_3(\mu\text{-}N,O\text{-}L^a)_2]$ molecule, the central Cu(II) ion has a square bipyramidal environment. The O_{hfac} atoms lie in the equatorial plane of the bipyramid (the Cu−O_{hfac} distances are 1.947(1) and 1.948(1) Å), and the
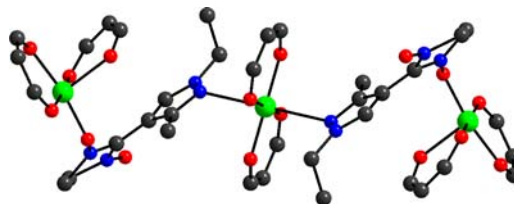

Figure 4. Molecular structure of $[[Cu(hfac)_2]_3(\mu\text{-}N,O\text{-}L^a)_2]$.
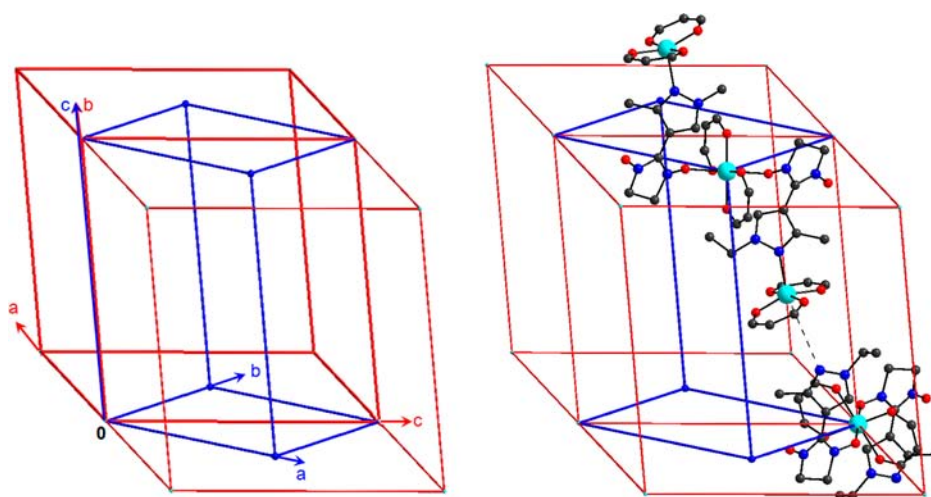
Figure 5. Relationship between the unit cell axes of the high- and low-temperature phases. The high-temperature cell is shown by red lines; its axes are designated by red letters. The low-temperature cell is shown by blue lines; its axes are designated by blue letters.

axial positions in it are occupied by the N atoms of the pyrazole rings of L^a (Cu−N 2.549(2) Å). The square pyramidal environment of the terminal Cu atoms is formed by the O atoms of the NO group (1.9320(15) Å) and hfac, one of which occupies the apex of the pyramid (Cu−O_{hfac} 1.924(2)− 1.952(2) and 2.206(2) Å). The intermolecular distances between the paramagnetic centers exceed 7 Å. The magnetic properties of $[[Cu(hfac)_2]_3(\mu\text{-}N,O\text{-}L^a)_2]$ are quite trivial. At 300 K, χT = 0.56 cm^3 K/mol, gradually decreasing to 0.46 cm^3 K/mol upon cooling at 10 K. This behavior of $\chi T(T)$ points to very strong (in energy) antiferromagnetic exchange interactions in the terminal $\{>N{-}{}^{\bullet}O{-}Cu^{2+}\}$ fragments of the molecule, as a result of which the main contribution to the moment is from the "central" Cu^{2+} ions of the trinuclear molecules.

CONCLUSIONS

The first example of a reversible single-crystal-to-single-crystal (SC−SC) reaction for a transition-metal complex with a stable organic radical initiated by variation of temperature has been reported. At room temperature, the molecular structure of $[[Cu(hfac)_2]_3(\mu\text{-}O,N\text{-}L^a)_2][Cu(hfac)_2(O\text{-}L^a)_2]$ is formed by the alternating fragments of the pair complex. Cooling the crystals of the complex below 225 K causes a significant displacement of adjacent molecules relative to each other, which ends with a transformation of the molecular structure into a polymer-chain structure. Repeated cooling−heating cycles in the solid actually lead to a reversible polymerization−depolymerization coordination reaction. The occurrence of polymerization on cooling is the result of the anomalously large shortening of intermolecular distances between the terminal Cu atoms of the $\{[[Cu(hfac)_2]_3(\mu\text{-}O,N\text{-}L^a)_2]\}$ trinuclear fragments and the non-coordinated N atoms of the pyrazole rings of the $\{[Cu(hfac)_2(O\text{-}L^a)_2]\}$ mononuclear fragments. When the low-temperature phase is heated above 270 K, the polymer-chain structure is destroyed and the compound is again transformed to a molecular pair complex. SC−SC transformations are rarely recorded, because they require high cooperativity and coherence of the intracrystalline motions of molecules. Examples of SC−SC polymerization initiated by the cooling of a coordination compound below room temperature are rare. Earlier, a SC−SC transformation of $[ZnCl_2(\mu\text{-bipy})]$ from a chain polymer to a two-dimensional network at low temper-

ature (<130 K) was reported.[40] To the best of our knowledge, the SC−SC transformation of a monomer complex into a chain polymer initiated by cooling a crystal below room temperature, reported here, has no analogues.

Figure 5 shows the relationship between the axes of the unit cell of the high- and low-temperature phases described by the transition matrix

$$
\begin{bmatrix}
-0.5 & 0 & 0.5 \\
0.5 & 0 & 0.5 \\
0 & 1 & 0
\end{bmatrix}
$$

Since the structural transformation caused an ensuing magnetic anomaly, the possibility of studying the structure of the compound before and after the transition was especially valuable for a reliable description of magnetostructural correlations. Repeated cooling−heating cycles led to considerable changes in the Cu−O_{NO} distances in the $\{>N{-}{}^{\bullet}O{-}Cu^{2+}{-}O^{\bullet}{-}N<\}$ exchange clusters, which caused changes in the value and sign of the exchange integral in the clusters. This was the reason for the jumps on the $\chi T(T)$ curve during repeated cooling−heating cycles. The temperature ranges of the magnetic effects were reproducible and corresponded to the structural transformation temperatures. The heterospin complex under study is actually another example of a compound that demonstrates the bistability effect.

ASSOCIATED CONTENT

Ⓢ Supporting Information

Structural parameters, crystal, and structure refinement data, atomic coordinates, and isotropic displacement parameters for both polymorphs of L^a, L^b, $[[Cu(hfac)_2]_3(\mu\text{-}O,N\text{-}L^a)_2][Cu(hfac)_2(O\text{-}L^a)_2]$, and $[[Cu(hfac)_2]_3(\mu\text{-}N,O\text{-}L^a)_2]$ (in CIF form); Tables S1−S3, Figure S1. These materials are available free of charge via Internet at http://pubs.acs.org.

AUTHOR INFORMATION

Corresponding Author

*E-mail: Victor.Ovcharenko@tomo.nsc.ru.

Notes

■ REFERENCES

(1) Lauher, J. W.; Fowler, F. W.; Goroff, N. S. *Acc. Chem. Res.* **2008**, *41*, 1215−1229.

(2) Tanaka, K.; Toda, F. *Chem. Rev.* **2000**, *100*, 1025−1074.

(3) Boldyreva, E.; Boldyrev, V. V. *Reactivity in Molecular Solids*; Wiley: Chichester, U.K., 1999.

(4) Turowska-Tyrk, I. *J. Phys. Org. Chem.* **2004**, *17*, 837−847.

(5) Reddy, C. M.; Krishna, G. R.; Ghosh, S. *CrystEngComm* **2010**, *12*, 2296−2314.

(6) Al-Kaysi, R. O.; Müller, A. M.; Bardeen, C. J. *J. Am. Chem. Soc.* **2006**, *128*, 15938−15939.

(7) Al-Kaysi, R. O.; Bardeen, C. J. *Adv. Mater.* **2007**, *19*, 1276−1280.

(8) Fernandes, M. A.; Levendis, D. C; Schoening, F. R. L. *Acta Crystallogr., Sect. B: Struct. Sci.* **2004**, *B60*, 300−314.

(9) Reddy, C. M.; Basavoju, S.; Desiraju, G. R. *Chem. Commun.* **2005**, 2439−2441.

(10) Reddy, C. M.; Kirchner, M. T.; Gundakaram, R. C.; Padmanabhan, K. A.; Desiraju, G. R. *Chem.−Eur. J.* **2006**, *12*, 2222−2234.

(11) Irie, M.; Kobatake, S.; Horichi, M. *Science* **2001**, *291*, 1769−1772.

(12) Kobatake, S.; Takami, S.; Muto, H.; Ishikawa, T.; Irie, M. *Nature* **2007**, *446*, 778−781.

(13) Reddy, C. M.; Gundakaram, R. C.; Basavoju, S.; Kirchner, M. T.; Padmanabhan, K. A.; Desiraju, G. R. *Chem. Commun.* **2005**, 3945−3947.

(14) Boese, R.; Cammack, J. K.; Matzger, A. J.; Pflug, K.; Tolman, W. B.; Vollhardt, K. P. C.; Weidman, T. W. *J. Am. Chem. Soc.* **1997**, *119*, 6757−6773.

(15) Massera, C.; Melegary, M.; Kalenius, E.; Ugozzoli, F.; Dalkanale, E. *Chem.−Eur. J.* **2011**, *17*, 3064−3068.

(16) Irie, M. *Chem. Rev.* **2000**, *100*, 1685−1716.

(17) Skoko, Ž.; Zamir, S.; Naumov, P.; Bernstein, J. *J. Am. Chem. Soc.* **2010**, *132*, 14191−14202.

(18) Morimoto, M.; Irie, M. *J. Am. Chem. Soc.* **2010**, *132*, 14172−14178.

(19) Naumov, P.; Kowalik, J.; Solntsev, K. M.; Baldridge, A.; Moon, J.-S.; Kranz, C.; Tolbert, L. M. *J. Am. Chem. Soc.* **2010**, *132*, 5845−5857.

(20) Garcia-Garibay, M. A. *Angew. Chem., Int. Ed.* **2007**, *46*, 8945−8947.

(21) Paul, I. C.; Curtin, D. Y. *Acc. Chem. Res.* **1973**, *6*, 217−225.

(22) Shalaev, E. Yu.; Zografi, G. *J. Phys. Org. Chem.* **1996**, *9*, 729−738.

(23) Lieberman, H. F.; Davey, R. J; Newsham, D. M. T. *Chem. Mater.* **2000**, *12*, 490−494.

(24) Bernshtein, J. *Polymorphism in Molecular Crystals*; Clarendon Press: Oxford, U.K., 2002.

(25) Chu, Q.; Swenson, D. C.; MacGillivray, L. R. *Angew. Chem., Int. Ed.* **2005**, *44*, 3569−3572.

(26) Vittal, J. J. *Coord. Chem. Rev.* **2007**, *251*, 1781−1795.

(27) Hao, Z.-M.; Zhang, X.-M. *Dalton Trans.* **2011**, *40*, 2092−2098.

(28) Cheng, X.-N.; Zhang, W.-X.; Chen, X.-M. *J. Am. Chem. Soc.* **2007**, *129*, 15738−15739.

(29) Zhang, Y.-J.; Liu, T.; Kanegawa, S.; Sato., O. *J. Am. Chem. Soc.* **2009**, *131*, 7942−7943.

(30) Bradshaw, D.; Warren, J. E.; Rosseinsky, M. J. *Science* **2007**, *315*, 977−980.

(31) Su, Z.; Chen, M.; Okamura, T.; Chen, M.-S.; Chen, S.-S.; Sun, W.-Y. *Inorg. Chem.* **2011**, *50*, 985−991.

(32) Kaneko, W.; Ohba, M.; Kitagawa, S. *J. Am. Chem. Soc.* **2007**, *129*, 13706−13712.

(33) Supriya, S.; Das, S. K. *J. Am. Chem. Soc.* **2007**, *129*, 3464−3465.

(34) Bezzu, C. G.; Helliwell, M.; Warren, J. E.; Allan, D. R.; McKeown, N. B. *Science* **2010**, *327*, 1627−1630.

(35) Albrecht, M.; Lutz, M.; Spek, A. L.; van Koten, G. *Nature* **2000**, *406*, 970−974.

(36) Huang, Z.; White, P. S.; Brookhart, M. *Nature* **2010**, *465*, 598−601.

(37) Zenkina, O. V.; Keske, E. C.; Wang, R.; Crudden, C. M. *Angew. Chem., Int. Ed.* **2011**, *50*, 8100−8104.

(38) Cheng, K.; Foxman, B. M. *J. Am. Chem. Soc.* **1977**, *99*, 8102−8103.

(39) Hu, C.; Englert, U. *Angew. Chem., Int. Ed.* **2006**, *45*, 3457−3459.

(40) Hu, C.; Englert, U. *Angew. Chem., Int. Ed.* **2005**, *44*, 2281−2283.

(41) Kahn, O. *Molecular Magnetism*; Wiley−VCH: New York, 1993.

(42) Stanovnik, B.; Svete, J. In *Science of Synthesis: Houben-Weyl Methods of Molecular Transformations*, Category 2, Vol. 12; Neier, R., Ed.; Georg Thieme Verlag: Stuttgart, Germany, and New York, 2002; pp 23−30.

(43) Ovcharenko, V. I.; Fokin, S. V.; Korobkov, I. V.; Rey, P. *Russ. Chem. Bull., Int. Ed.* **1999**, *48*, 1519−1525.

(44) Hirel, C.; Vostrikova, K. E.; Pécaut, J.; Ovcharenko, V. I.; Rey, P. *Chem.−Eur. J.* **2001**, *7*, 2007−2014.

(45) van Auwers, K.; Hollmann, H. *Chem. Ber.* **1926**, *59*, 1282−1302.

(46) Ovcharenko, V. I.; Fokin, S. V.; Romanenko, G. V.; Shvedenkov, Yu. G.; Ikorskii, V. N.; Tretyakov, E. V.; Vasilevsky, S. F. *Russ. J. Struct. Chem.* **2002**, *43*, 153−167.

(47) Kukharev, B. F.; Stankevich, V. K.; Lobanova, N. A.; Sadykov, E. Kh.; Kukhareva, V. A. *Russ. J. Org. Chem.* **2006**, *42*, 1568−1569.

(48) *Cambridge Structural Database*, version 5.33; Cambridge Crystallographic Data Centre: Cambridge, U.K., Nov. 2011 (last updated Feb. 2012).

(49) Veber, S. L.; Fedin, M. V.; Potapov, A. I.; Maryunina, K. Yu.; Romanenko, G. V.; Sagdeev, R. Z.; Ovcharenko, V. I.; Goldfarb, D.; Bagryanskaya, E. G. *J. Am. Chem. Soc.* **2008**, *130*, 2444−2445.

(50) Sorai, M.; Ensling, J.; Hasselbach, K. M.; Gütlich, P. *Chem. Phys.* **1977**, *20*, 197−208.

(51) Gütlich, P.; Köppen, H.; Steinhäuser, H. G. *Chem. Phys. Lett.* **1980**, *74*, 475−480.

(52) Gütlich, P.; Hauser, A.; Spiering, H. *Angew. Chem., Int. Ed. Engl.* **1994**, *33*, 2024−2054.

(53) Murray, K. S.; Kepert, C. J. *Top. Curr. Chem.* **2004**, *233*, 216−219.

(54) Sorai, M. *Top. Curr. Chem.* **2004**, *235*, 151−161.

(55) Katz, B. A.; Strouse, C. E. *J. Am. Chem. Soc.* **1979**, *101*, 6214−6221.

(56) Greenaway, A. M.; Sinn, E. *J. Am. Chem. Soc.* **1978**, *100*, 8080−8084.

(57) Greenaway, A. M.; O'Connor, C. J.; Schrock, A.; Sinn, E. *Inorg. Chem.* **1979**, *18*, 2692−2695.

(58) Wiehl, L.; Kiel, G.; Köhler, C. P.; Spiering, H.; Gütlich, P. *Inorg. Chem.* **1986**, *25*, 1565−1571.

(59) Hostettler, M.; Törnroos, K. W.; Chernyshov, D.; Vangdal, B.; Bürgi, H.-B. *Angew. Chem., Int. Ed.* **2004**, *43*, 4589−4594.

(60) Halder, G. J.; Kepert, C. J.; Moubaraki, B.; Murray, K. S.; Cashion, J. D. *Science* **2002**, *298*, 1762−1765.

(61) Neville, S. M.; Halder, G. J.; Chapman, K. W.; Duriska, M. B.; Southon, P. D.; Cashion, J. D.; Létard, J.-F.; Moubaraki, B.; Murray, K. S.; Kepert, C. J. *J. Am. Chem. Soc.* **2008**, *130*, 2869−2876.